

Generation of Terahertz Radiation by Hot Electrons in Carbon Nanotubes

O. V. Kibis

Department of Applied and Theoretical Physics, Novosibirsk State Technical University, Novosibirsk 630092, Russia

M. Rosenau da Costa

International Center for Condensed Matter Physics, University of Brasilia, 70904-970 Brasilia DF, Brazil

M. E. Portnoi*

School of Physics, University of Exeter, Stocker Road, Exeter EX4 4QL, United Kingdom

Received July 27, 2007; Revised Manuscript Received October 14, 2007

ABSTRACT

We demonstrate theoretically that quasi-metallic carbon nanotubes emit terahertz radiation induced by an applied voltage. It is shown that in the ballistic transport regime their spontaneous emission spectra have a universal frequency and bias voltage dependence, which raises the possibility of utilizing this effect for high-frequency nanoelectronic devices.

Creating a compact reliable source of terahertz (THz) radiation is one of the most formidable tasks of contemporary applied physics.^{1,2} One of the latest trends in THz technology³ is to use carbon nanotubes, cylindrical molecules with nanometer diameter and micrometer length,^{4–7} as building blocks of high-frequency devices. There are several promising proposals of using carbon nanotubes for THz applications including a nanoklystron utilizing extremely efficient high-field electron emission from nanotubes,^{3,8,9} devices based on negative differential conductivity in large-diameter semiconducting nanotubes,^{10,11} high-frequency resonant-tunneling diodes¹² and Schottky diodes,^{13–16} as well as electric-field-controlled carbon nanotube superlattices,¹⁷ frequency multipliers,^{18,19} THz amplifiers,²⁰ switches,²¹ and antennas.²²

In this letter, we propose an alternative scheme for generating THz radiation from single-walled carbon nanotubes (SWNTs). This scheme is based on the electric-field-induced heating of an electron gas, resulting in the inversion of population of optically active states with energy difference within the THz spectrum range. It is well known that the elastic backscattering processes in metallic SWNTs are strongly suppressed,^{23,24} and in a high enough electric field charge carriers can be accelerated up to the energy allowing emission of optical/zone-boundary phonons. At this energy,

corresponding to the frequency of about 40 THz, the major scattering mechanism switches on abruptly resulting in current saturation.^{25–28} In what follows, we show that for certain types of carbon nanotubes the heating of electrons to energies below the high-energy phonon emission threshold results in spontaneous THz emission with peak frequency controlled by an applied voltage.

The electron energy spectrum of metallic SWNTs, $\varepsilon(k)$, linearly depends on the electron wave vector k close to the Fermi energy and has the form $\varepsilon(k) = \pm \hbar v_F |k - k_0|$, where $v_F \approx 9.8 \times 10^5$ m/s is the Fermi velocity of graphene, which corresponds to the commonly used tight-binding matrix element $\gamma_0 = 3.033$ eV.^{4–6} Here and in what follows, the zero of energy is defined as the Fermi energy position in the absence of an external field. When the voltage, V , is applied between the SWNT ends, the electron distribution is shifted in the way shown by the heavy lines in Figure 1 corresponding to the filled electron states. This shift results in inversion of population and, correspondingly, in optical transitions between filled states in the conduction band and empty states in the valence band. The spectrum of optical transitions is determined by the distribution function for hot carriers, which in turn depends on the applied voltage and scattering processes in the SWNT. In high-quality nanotubes, disorder-mediated scattering is known to be weaker than electron–phonon scattering.^{25–28} Because the scattering

* Corresponding author. E-mail: m.e.portnoi@exeter.ac.uk.

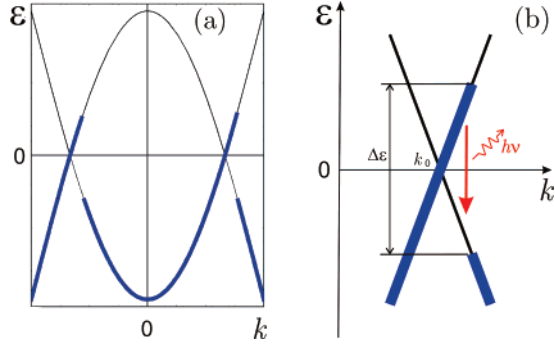


Figure 1. (a) Crossing valence and conduction subbands in metallic SWNTs. Thick lines show the states occupied by electrons in the presence of an applied bias voltage. (b) The scheme of THz photon generation by hot carriers.

processes erode the inversion of electron population, an optimal condition for observing the discussed optical transitions takes place when the length of the SWNT $L < l_{ac}$, where the electron mean-free path for acoustic phonon scattering is $l_{ac} \approx 2.4 \mu\text{m}$.²⁷ Below, we consider only such short SWNTs in the ballistic transport regime when the total shift, $\Delta\epsilon$, of electron distribution (see Figure 1b) does not exceed the value of $\hbar\Omega = 0.16 \text{ eV}$ at which the fast emission of high-energy phonons begins.²⁷ This shift is related to the current, I , running through the nanotube by the Büttiker–Landauer type formula, $\Delta\epsilon = (\hbar/4e)I$, and it cannot exceed the value of eV with $\Delta\epsilon \rightarrow eV$ in case of ideal Ohmic contacts,²⁶ which we will suppose from now on. In the ballistic or so-called “low-bias” regime,^{26,27} which persists for submicron SWNTs for applied voltages up to $V \approx 0.16 \text{ V}$, the distribution function for hot electrons is

$$f_e(k) = \begin{cases} 1, & 0 < k - k_0 < \Delta\epsilon/2\hbar v_F \\ 0, & k - k_0 > \Delta\epsilon/2\hbar v_F \end{cases} \quad (1)$$

The distribution function for hot holes, $f_h(k)$, has the same form as $f_e(k)$.

Let us select a SWNT with the crystal structure most suitable for observation of THz emission from a biased nanotube. First, the required nanotube should have metallic conductivity, and second the optical transitions between the lowest conduction subband and the top valence subband should be allowed. The crystal structure of a SWNT is described by two integers (n, m) , which completely define the nanotube physical properties.^{4–6} The SWNTs with true metallic energy band structure, for which the energy gap is absent for any SWNT radius, are the armchair (n, n) SWNTs only.^{6,29–32} However, for armchair SWNTs the optical transitions between the first conduction and valence subbands are forbidden.^{33,34} Therefore, we propose to use for the observation of THz generation the so-called quasi-metallic (n, m) SWNTs with $n - m = 3p$, where p is a nonzero integer. These nanotubes, which are gapless within the frame of a simple zone-folding model of the π -electron graphene

spectrum,⁴ are in fact narrow-gap semiconductors due to curvature effects. Their band gap is given by^{29,32}

$$\epsilon_g = \frac{\hbar v_F a_{C-C} \cos 3\theta}{8R^2} \quad (2)$$

where $a_{C-C} = 1.42 \text{ \AA}$ is the nearest-neighbor distance between two carbon atoms, R is the nanotube radius, and $\theta = \arctan[3m/(2n + m)]$ is the chiral angle.⁴ It can be seen from eq 2 that the gap is decreasing rapidly with increasing nanotube radius. For large values of R , this gap can be neglected even in the case of moderate applied voltages due to Zener tunneling of electrons across the gap. It is easy to show in a fashion similar to Zener’s original work³⁵ that the tunneling probability in quasi-metallic SWNTs is given by $\exp(-\alpha\epsilon_g^2/eE\hbar v_F)$, where α is a numerical factor close to unity.³⁶ For example, for a zigzag $(30, 0)$ SWNT the gap is $\epsilon_g \approx 6 \text{ meV}$, and the Zener breakdown takes place for the electric field $E \sim 10^{-1} \text{ V}/\mu\text{m}$. Because almost the whole voltage drop in the ballistic regime occurs within the few nanometer regions near the contacts,^{7,37} a typical 0.1 V bias voltage corresponds to an electric field more than sufficient to achieve a complete breakdown. In what follows, we present explicit results for a zigzag $(3p, 0)$ SWNT of large enough radius R and for applied bias exceeding the Zener breakdown voltage so that the finite-gap effects can be neglected. These results can be easily generalized for any quasi-metallic large radius SWNT.

Optical transitions in SWNTs have been a subject of extensive research (see, e.g., refs 33, 34, 38–42; comprehensive reviews of earlier work can be found in refs 5, 6). We treat them using the nearest-neighbor orthogonal π -electron tight-binding model.⁴ Despite its apparent simplicity and well-known limitations, this model has been extremely fruitful in describing low-energy optical spectra and electronic properties of SWNTs (see, e.g., ref 43). Our goal is to calculate the spectral density of spontaneous emission, I_ν , which is the probability of optical transitions per unit time with photon frequencies in the interval $(\nu, \nu + d\nu)$ divided by $d\nu$. In the dipole approximation,⁴⁴ this spectral density is given by

$$I_\nu = \frac{8\pi e^2 \nu}{3c^3} \sum_{if} f_e(k_i) f_h(k_f) |\langle \Psi_f | \hat{v}_z | \Psi_i \rangle|^2 \delta(\epsilon_i - \epsilon_f - \hbar\nu) \quad (3)$$

Equation 3 contains the matrix element of the electron velocity operator. In the frame of the tight-binding model, this matrix element for optical transitions between the lowest conduction and the highest valence subbands of the $(3p, 0)$ zigzag SWNT can be written as (cf. refs 34, 38)

$$\langle \Psi_f | \hat{v}_z | \Psi_i \rangle = \frac{a_{C-C} \omega_{if}}{8} \delta_{k_p k_i} \quad (4)$$

where $\hbar\omega_{if} = \epsilon_i - \epsilon_f$ is the energy difference between the initial (i) and the final (f) states. These transitions are

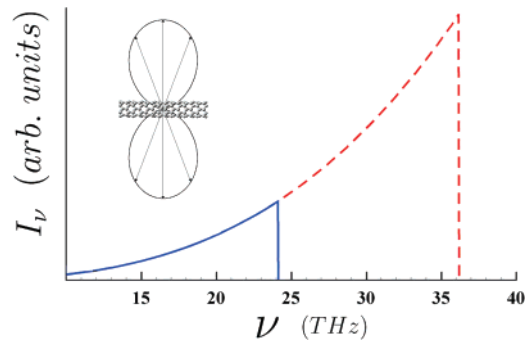


Figure 2. The spectral density of spontaneous emission as a function of frequency for two values of applied voltage: solid line for $V = 0.1$ V; dashed line for $V = 0.15$ V. The inset shows the directional radiation pattern of the THz emission with respect to the nanotube axis.

associated with light polarized along the nanotube axis z in agreement with the general selection rules for SWNTs.³³ Substituting eq 4 in eq 3 and performing necessary summation, we get

$$I_\nu = L f_e(\pi\nu/v_F) f_h(\pi\nu/v_F) \frac{\pi^2 e^2 a_{C-C}^2 \nu^3}{6c^3 \hbar v_F} \quad (5)$$

Equation 5 has broader applicability limits than the considered case of $L < l_{ac}$ and $eV < \hbar\Omega$ in which the distribution functions for electrons and holes are given by eq 1. In the general case, there is a strong dependence of I_ν on the distribution functions, which have to be calculated taking into account all the relevant scattering mechanisms.^{25–28,37,45} Our calculations show that for any nonzigzag quasi-metallic SWNT the frequency dependence of the matrix element of the velocity operator remains linear, differing from eq 4 only by a geometrical factor. Consequently, in the discussed ballistic regime the spectral density has a universal dependence on the applied voltage and photon frequency for all quasi-metallic SWNTs. In Figure 2 the spectral density is shown for two values of the voltage. It is clearly seen that the maximum of the spectral density of emission has a strong voltage dependence and lies in the THz frequency range for experimentally attainable voltages. Spectrally integrating I_ν yields the total photon emission rate. For a single zigzag SWNT with length $L = 2 \mu\text{m}$ and applied voltage of 0.16 V, this rate is approximately 3000 photons per second. This number can be significantly increased for an array⁴⁶ of similarly biased nanotubes for which stimulated emission will occur.

The directional radiation pattern, shown in the inset of Figure 2, is given by $\cos^2 \varphi$, where φ is the angle between the light propagation direction and the nanotube axis. It reflects the fact that the emission of light polarized normally to the nanotube axis is forbidden by the selection rules for optical transitions between the lowest conduction subband and the top valence subband. For some device applications, it might be desirable to emit photons propagating along the nanotube axis, which is possible in optical transitions between the SWNT subbands characterized by angular

momenta differing by one.^{6,33} To achieve the emission of these photons by the electron heating, it is necessary to have an intersection of such subbands within the energy range accessible to electrons accelerated by attainable voltages. From our analysis of different types of SWNTs, it follows that the intersection is possible, for example, for the lowest conduction subbands in several semiconducting zigzag nanotubes and in all armchair nanotubes. However, for an effective THz emission from these nanotubes it is necessary to move the Fermi level very close to the subband intersection point.⁴⁷ Therefore, obtaining THz emission propagating along the nanotube axis is a much more difficult technological problem compared to the generation of the emission shown in Figure 2.

In conclusion, we have demonstrated that a quasi-metallic carbon nanotube can emit THz radiation when a potential difference is applied to its ends. The typical required voltages and nanotube parameters are similar to those available in the state-of-the-art transport experiments. The maximum of the spectral density of emission is shown to have a strong voltage dependence, which is universal for all quasi-metallic carbon nanotubes in the ballistic regime. Therefore, the discussed effect can be used for creating a THz source with frequency controlled by the applied voltage. Appropriately arranged arrays of the nanotubes should be considered as promising candidates for active elements of amplifiers and generators of coherent THz radiation. In such an array, all biased quasi-metallic SWNTs will emit in a similar fashion, whereas semiconducting and armchair nanotubes will be optically inactive in the THz and mid-infrared range; therefore, no special selection of the nanotube type is needed. In addition, the discussed effect provides a spectroscopic tool allowing us to distinguish between quasi-metallic and true metallic (armchair) nanotubes and to verify the validity of the ballistic transport picture for short SWNTs at elevated temperatures and nonvanishing bias voltages.

Acknowledgment. The work was supported by INTAS (Grants 03-50-4409 and 05-1000008-7801), the Russian Foundation for Basic Research (Grants 06-02-16005, 06-02-81012, and 08-02-90004), the Russian Ministry for Education and Science (Grant RNP.2.1.1.1604), the Royal Society (UK), MCT, and IBEM (Brazil). O.V.K. and M.E.P. are grateful to the ICCMP staff for hospitality.

References

- (1) Lee, M.; Wanke, M. C. *Science* **2007**, *316*, 64.
- (2) Ferguson, B.; Zhang, X. C. *Nat. Mater.* **2002**, *1*, 26.
- (3) Dragoman, D.; Dragoman, M. *Prog. Quantum Electron.* **2004**, *28*, 1.
- (4) Saito, R.; Dresselhaus, G.; Dresselhaus, M. S. *Physical Properties of Carbon Nanotubes*; Imperial College Press: London, 1998.
- (5) *Carbon Nanotubes: Synthesis, Structure, Properties, and Applications*; Dresselhaus, M. S., Dresselhaus, G., Avouris, Ph., Eds.; Springer-Verlag: Berlin, 2001.
- (6) Reich, S.; Thomsen, C.; Maultzsch, J. *Carbon Nanotubes: Basic Concepts and Physical Properties*; Wiley: Berlin, 2004.
- (7) Anantram, M. P.; Léonard, F. *Rep. Prog. Phys.* **2006**, *69*, 507.
- (8) Manohara, H. M.; Bronikowski, M. J.; Hoenk, M.; Hunt, B. D.; Siegel, P. H. *J. Vac. Sci. Technol., B* **2005**, *23*, 157.
- (9) Di Carlo, A.; Pecchina, A.; Petrolati, E.; Paolini, C. *Proc. SPIE-Int. Soc. Opt. Eng.* **2006**, *6328*, 632808.

- (10) Maksimenko, A. S.; Slepyan, G. Ya. *Phys. Rev. Lett.* **2000**, *84*, 362.
- (11) Pennington, G.; Goldsman, N. *Phys. Rev. B* **2003**, *68*, 045426.
- (12) Dragoman, D.; Dragoman, M. *Physica E* **2004**, *24*, 282.
- (13) Odintsov, A. A. *Phys. Rev. Lett.* **2000**, *85*, 150.
- (14) Léonard, F.; Tersoff, J. *Phys. Rev. Lett.* **2000**, *85*, 4767.
- (15) Yang, M. H.; Teo, K. B. K.; Milne, W. I.; Hasko, D. G. *Appl. Phys. Lett.* **2005**, *87*, 253116.
- (16) Lu, C.; An, L.; Fu, Q.; Liu, J.; Zhang, H.; Murduck, J. *Appl. Phys. Lett.* **2006**, *88*, 133501.
- (17) Kibis, O. V.; Parfitt, D. G. W.; Portnoi, M. E. *Phys. Rev. B* **2005**, *71*, 035411.
- (18) Slepyan, G. Ya.; Maksimenko, S. A.; Kalosha, V. P.; Herrmann, J.; Campbell, E. E. B.; Hertel, I. V. *Phys. Rev. A* **1999**, *60*, R777.
- (19) Slepyan, G. Ya.; Maksimenko, S. A.; Kalosha, V. P.; Gusakov, A. V.; Herrmann, J. *Phys. Rev. A* **2001**, *63*, 053808.
- (20) Dragoman, D.; Dragoman, M. *Physica E* **2005**, *25*, 492.
- (21) Dragoman, M.; Cismaru, A.; Hartnagel, H.; Plana, R. *Appl. Phys. Lett.* **2006**, *88*, 073503.
- (22) Slepyan, G. Ya.; Shuba, M. V.; Maksimenko, S. A.; Lakhtakia, A. *Phys. Rev. B* **2006**, *73*, 195416.
- (23) Ando, T.; Nakanishi, T.; Saito, R. *J. Phys. Soc. Jpn.* **1997**, *67*, 1704.
- (24) Roche, S.; Triozon, F.; Rubio, A. *Appl. Phys. Lett.* **2001**, *79*, 3690.
- (25) Yao, Z.; Kane, C. L.; Dekker, C. *Phys. Rev. Lett.* **2000**, *84*, 2941.
- (26) Javey, A.; Guo, J.; Paulsson, M.; Wang, Q.; Mann, D.; Lundstrom, M.; Dai, H. *Phys. Rev. Lett.* **2004**, *92*, 106804.
- (27) Park, J.-Y.; Resenblatt, S.; Yaish, Yu.; Sazonova, V.; Üstünel, H.; Braig, S.; Arias, T. A.; Brouwer, P. W.; McEuen, P. L. *Nano Lett.* **2004**, *4*, 517.
- (28) Perebeinos, V.; Tersoff, J.; Avouris, P. *Phys. Rev. Lett.* **2005**, *94*, 086802.
- (29) Kane, C. L.; Mele, E. J. *Phys. Rev. Lett.* **1997**, *78*, 1932.
- (30) Ouyang, M.; Huang, J.-L.; Cheung, C. L.; Lieber, C. M. *Science* **2001**, *292*, 702.
- (31) Li, Y.; Ravaoli, U.; Rotkin, S. V. *Phys. Rev. B* **2006**, *73*, 035415.
- (32) Gunlycke, D.; Lambert, C. J.; Bailey, S. W. D.; Pettifor, D. G.; Briggs, G. A. D.; Jefferson, J. H. *Europhys. Lett.* **2006**, *73*, 759.
- (33) Milošević, I.; Vuković, T.; Dmitrović, S.; Damnjanović, M. *Phys. Rev. B* **2003**, *67*, 165418.
- (34) Jiang, J.; Saito, R.; Grüneis, A.; Dresselhaus, G.; Dresselhaus, M. S. *Carbon* **2004**, *42*, 3169.
- (35) Zener, C. *Proc. R. Soc. London* **1934**, *145*, 523.
- (36) For the energy spectrum near the band edge given by $\varepsilon = \pm[\varepsilon_g^2/4 + \hbar^2 v_F^2 (k - k_0)^2]^{1/2}$, it can be shown that $\alpha = \pi/4$.
- (37) Svizhenko, A.; Anantram, M. P. *Phys. Rev. B* **2005**, *72*, 085430.
- (38) Grüneis, A.; Saito, R.; Samsonidze, G. G.; Kimura, T.; Pimenta, M. A.; Joria, A. A.; Souza Filho, G.; Dresselhaus, G.; Dresselhaus, M. S. *Phys. Rev. B* **2003**, *67*, 165402.
- (39) Popov, V. N.; Henrard, L. *Phys. Rev. B* **2004**, *70*, 115407.
- (40) Saito, R.; Grüneis, A.; Samsonidze, G. G.; Dresselhaus, G.; Dresselhaus, M. S.; Jorio, A.; Cançado, L. G.; Pimenta, M. A.; Souza Filho, A. G. *Appl. Phys. A* **2004**, *78*, 1099.
- (41) Goupalov, S. V. *Phys. Rev. B* **2005**, *72*, 195403.
- (42) Oyama, Y.; Saito, R.; Sato, K.; Jiang, J.; Samsonidze, G. G.; Grüneis, A.; Miyauchi, Y.; Maruyama, S.; Jorio, A.; Dresselhaus, G.; Dresselhaus, M. S. *Carbon* **2006**, *44*, 873.
- (43) Sfeir, M. Y.; Beetz, T.; Wang, F.; Huang, L.; Huang, X. M. H.; Huang, M.; Hone, J.; O'Brien, S.; Misewich, J. A.; Heinz, T. F.; Wu, L.; Zhu, Y.; Brus, L. E. *Science* **2006**, *312*, 554.
- (44) Berestetskii, V. B.; Lifshitz, E. M.; Pitaevskii, L. P. *Quantum Electrodynamics*; Butterworth-Heinemann: Oxford, MA, 1997.
- (45) Kuroda, M. A.; Cangellaris, A.; Leburton, J.-P. *Phys. Rev. Lett.* **2005**, *95*, 266803.
- (46) Hata, K.; Futaba, D. N.; Mizuno, K.; Namai, T.; Yumura, M.; Iijima, S. *Science* **2004**, *306*, 1362.
- (47) Kibis, O. V.; Portnoi, M. E. *Tech. Phys. Lett.* **2005**, *31*, 671.

NL0718418